0026-895X/09/7605-1019–1030$20.00
MOLECULAR PHARMACOLOGY
Copyright © 2009 The American Society for Pharmacology and Experimental Therapeutics
Mol Pharmacol 76:1019–1030, 2009

Vol. 76, No. 5
58651/3530723
Printed in U.S.A.

Interactions of Histamine H_1-Receptor Agonists and Antagonists with the Human Histamine H_4-Receptor

Karl-Friedrich Deml, Silke Beermann, Detlef Neumann, Andrea Strasser, and Roland Seifert

Departments of Pharmacology and Toxicology (K.-F.D.) and Pharmaceutical/Medicinal Chemistry I (A.S.), School of Pharmacy, University of Regensburg, Regensburg, Germany; and Institute of Pharmacology, Medical School of Hannover, Hannover, Germany (S.B., D.N., R.S.)

Received June 17, 2009; accepted August 31, 2009

ABSTRACT

The human histamine H_4-receptor (hH_4R) possesses high constitutive activity and, like the human H_1-receptor (hH_1R), is involved in the pathogenesis of type-I allergic reactions. The study aims were to explore the value of dual H_1/H_4R antagonists as antiallergy drugs and to address the question of whether H_1R ligands bind to hH_4R. In an acute murine asthma model, the H_1R antagonist mepyramine and the H_4R antagonist 1-[(5-chloro-1*H*-indol-2-yl)carbonyl]-4-methyl-piperazine (JNJ 7777120) exhibited synergistic inhibitory effects on eosinophil accumulation in the bronchoalveolar lavage fluid. At the hH_4R expressed in Sf9 insect cells, 18 H_1R antagonists and 22 H_1R agonists showed lower affinity to hH_4R than to hH_1R as assessed in competition binding experiments. For a small number of H_1R antagonists, hH_4R partial agonism was observed in the steady-state GTPase assay. Most compounds were neutral antagonists or inverse agonists. Twelve phenylhistamine-type hH_1R partial agonists were also hH_4R partial agonists. Four histaprodifen-type hH_1R partial agonists were hH_4R inverse agonists. Dimeric histaprodifen was a more efficacious hH_4R inverse agonist than the reference compound thioperamide. Suprahistaprodifen was the only histaprodifen acting as hH_4R partial agonist. Suprahistaprodifen was docked into the binding pocket of inactive and active hH_4R models in two different orientations, predominantly stabilizing the active state of hH_4R. Collectively, the synergistic effects of H_1R and H_4R antagonists in an acute asthma model and the overlapping interaction of structurally diverse H_1R ligands with hH_1R and hH_4R indicate that the development of dual H_1R/H_4R antagonists is a worthwhile and technically feasible goal for the treatment of type-I allergic reactions.

Histamine is a neurotransmitter and local mediator and regulates numerous cell functions. Histamine mediates its effects through histamine receptors, belonging to the family of G protein-coupled receptors (GPCRs) (Foord et al., 2005): the histamine H_1 receptor (H_1R) (Moguilevsky et al., 1994), the histamine H_2 receptor (H_2R) (Gantz et al., 1991), the histamine H_3 receptor (H_3R) (Lovenberg et al., 1999), and the histamine H_4 receptor (H_4R) (Oda et al., 2000). The H_1R is involved in the pathogenesis of type I allergic diseases such as conjunctivitis and rhinitis; the H_2R is responsible for stimulation of gastric acid secretion; the H_3R is responsible for modulation of neurotransmitter release; the H_4R is involved in the pathogenesis of itching, autoimmune diseases such as rheumatoid arthritis, and type I allergic diseases such as bronchial asthma, conjunctivitis, and rhinitis (Thurmond et al., 2008). Although histamine binds to all four histamine receptors, the identity of amino acid sequences between H_1R, H_2R, H_3R, and H_4R is rather low, amounting to just 15 to 35% (Thurmond et al., 2008).

Thioperamide is a high-affinity antagonist/inverse agonist for H_3R and H_4R but possesses only low affinity for H_1R and H_2R. JNJ 7777120 is a high-affinity H_4R antagonist and exhibits only low affinity for H_1R, H_2R, and H_3R (Venable and Thurmond, 2006). Because not only the H_1R but also H_4R is involved in the pathogenesis of type I allergic diseases, dual H_1R/H_4R antagonism could constitute a more efficient antiallergy therapy than H_1R or H_4R antagonists alone (Thurmond et al., 2008). Unfortunately, there is a controversial and as-yet-unresolved discussion regarding whether H_1R antagonists posses low or high affinity for the H_4R (Nguyen et al., 2001; Lim et al., 2005; Venable and Thurmond, 2006). However, for the development of dual $H_1R/$

This work was supported by the Research Training Program (Graduiertenkolleg) GRK760 "Medicinal Chemistry: Molecular Recognition—Ligand-Receptor Interactions" of the Deutsche Forschungsgemeinschaft.
Article, publication date, and citation information can be found at http://molpharm.aspetjournals.org.
doi:10.1124/mol.109.058651.

ABBREVIATIONS: GPCR, G protein-coupled receptor; h, human; $h\beta_2AR$, human β_2-adrenoceptor; H_1R, histamine H_1 receptor; H_2R, histamine H_2 receptor; H_3R, histamine H_3 receptor; H_4R, histamine H_4 receptor; JNJ 7777120, 1-[(5-chloro-1*H*-indol-2-yl)carbonyl]-4-methyl-piperazine; MD, molecular dynamics; RGS19, regulator of G-protein signaling (GTPase activating protein) 19; TM, transmembrane domain; PBS, phosphate-buffered saline.

H_4R antagonists, it is important to clarify this important issue.

hH_4R exhibits high agonist-independent (i.e., constitutive) activity, resulting in high basal G-protein activity (Schneider et al., 2009). In the framework of the two-state model of GPCR activation, high constitutive activity of hH_4R is explained by a high spontaneous isomerization rate of hH_4R from the inactive (R) state to the active (R*) state (Seifert and Wenzel-Seifert, 2002). Inverse agonists stabilize the R state of GPCRs and reduce agonist-independent basal G-protein activity (Seifert and Wenzel-Seifert, 2002). Meanwhile, numerous H_4R antagonists (Jablonowski et al., 2003; Terzioglu et al., 2004; Venable et al., 2005; Smits et al., 2008) and agonists (Hashimoto et al., 2003; Lim et al., 2005; Igel et al., 2009) have been identified. Although thioperamide is commonly used as the reference hH_4R inverse agonist (Lim et al., 2005; Thurmond et al., 2008), the ligand is actually only a partial inverse agonist (Schneider et al., 2009). Highly efficacious hH_4R inverse agonists may be superior to hH_4R neutral antagonists in the treatment of type I allergic diseases (Schneider et al., 2009).

The aims of this study were to explore the value of dual H_1/H_4R antagonists as antiallergy drugs and to examine the interaction of H_1R ligands with hH_4R. To achieve the first aim, we examined the effects of the H_1R antagonist mepyramine (**3**) (Fig. 1) and the H_4R antagonist JNJ 7777120 (**43**) (Fig. 2) alone and in combination in an acute murine asthma model (Dunford et al., 2006). To achieve the second aim, we systematically examined 18 H_1R antagonists (Fig. 1) and 22 H_1R agonists (Fig. 2) at hH_4R expressed in Sf9 insect cells. We were particularly interested in identifying similarities and differences in the pharmacological profile of these compounds between hH_1R and hH_4R in the context of the amino acid sequences of hH_1R and hH_4R and the known ligand interaction sites in these GPCRs (Fig. 3). We included structurally diverse H_1R antagonists of the first and second generation as well as antidepressants, acting also as H_1R antagonists, into our study (**1**-**18**). Moreover, we characterized small H_1R agonists (**19**-**24**) and H_1R agonists of the phenylhistamine (**25**-**36**) and histaprodifen (**37**-**41**) classes (Leschke et al., 1995; Kramer et al., 1998; Elz et al., 2000; Menghin et al., 2003) at hH_4R.

Suprahistaprodifen binds to H_1R in two different orientations (Strasser et al., 2008a). To obtain more detailed insight onto the interactions of suprahistaprodifen with hH_4R, we generated a homology model of the inactive hH_4R based on the crystal structure of the human β_2AR (Cherezov et al., 2007; Rasmussen et al., 2007; Rosenbaum et al., 2007) and performed restrained molecular dynamics simulations to generate an active state model of hH_4R.

Materials and Methods

Materials. Ovalbumin (purity >98%; EndoGrade) was obtained from Hyglos (Regensburg, Germany) and dissolved at a concentration of 1 mg/ml in PBS, pH 7.4. [γ-^{32}P]GTP was synthesized as described previously (Preuss et al., 2007). [^{3}H]Histamine (14.2 Ci/mmol) was from PerkinElmer Life and Analytical Sciences (Waltham, MA). Sources of biochemical reagents were described previously (Seifert et al., 2003; Strasser et al., 2008a, 2009; Schneider et al., 2009). Chemical structures of the analyzed compounds are given in Figs. 1 and 2. Phenylhistamines and histaprodifens were dissolved as described previously (Seifert et al., 2003; Strasser et al., 2008a, 2009). Stock solutions of astemizole, azelastine, terfenadine, fexofenadine, ketotifen, clemastine, cyproheptadine, mirtazapine, and loratadine (10 mM each) were dissolved in dimethyl sulfoxide. In all assays with compounds dissolved in dimethyl sulfoxide, the dimethyl sulfoxide concentration was adjusted to 5% (v/v) to ensure complete dissolution of compounds and comparable assay conditions (Strasser et al., 2008a, 2009).

Acute Murine Asthma Model. Acute asthma in mice was induced according to a standard procedure (Dunford et al., 2006). In brief, female BALB/c mice (6–8 weeks old) were obtained from Janvier (Le Genest, France) and housed in the animal care unit of the Medical School of Hannover with a 12-h dark/light cycle and standard food and water ad libitum. At day 1 and 14, animals were sensitized by injection of 10 μg of ovalbumin i.p. adsorbed to 1.5 mg of aluminum hydroxide. Mice were injected with 0.1 ml of DMSO s.c. (control), 20 mg/kg mepyramine, 20 mg/kg JNJ 7777120, or a combination of 20 mg/kg mepyramine plus 20 mg/kg JNJ 7777120 30 min before and 2 h after the sensitization with ovalbumin at days 1 and 14. At days 21 to 24, animals were placed into a Plexiglas box and exposed for 20 min to an aerosol consisting of 1% (m/v) ovalbumin dissolved in PBS, pH 7.4. At day 25, mice were sacrificed by a lethal dose of xylazine (Rompun)/ketamine (ratio 2:3), and bronchoalveolar lavage was performed two times with 1.0 ml of PBS, pH 7.4. Differential leukocyte counts were performed by counting 400 cells stained with Diff-Quik (Medion Diagnostics, Düdingen, Switzerland) on cytospin preparations by light microscopy using standard morphological criteria. The effects of antagonists on eosinophil cell counts were compared with each other and the control group using one-way analysis of variance, Bartelett's test for equal variances and Bonferroni's multiple comparison test. The animal experiments were performed according to the German animal protection law and were approved by the animal protection committee of the Medical School of Hannover (file 33.9-42502-04-08/1550).

Pharmacological Assays with Sf9 Cell Membranes. Cell culture, generation of recombinant baculoviruses, and membrane preparations were performed as described previously (Strasser et al., 2008a; Schneider et al., 2009). The determination of protein concentration was performed as described previously (Seifert et al., 2003; Strasser et al., 2008a). The competition binding assays with Sf9 membranes, expressing hH_4R-RGS19, $G\alpha_{i2}$, and $G\beta_1\gamma_2$ were performed in presence of 10 nM [^{3}H]histamine as described previously (Schneider and Seifert, 2009). Nonspecific [^{3}H]histamine binding amounted to <25% of total [^{3}H]histamine binding and was determined in the presence of 10 mM thioperamide (**42**). The steady-state GTPase assays with Sf9 membranes coexpressing hH_4R-RGS19 with $G\alpha_{i2}$ and $G\beta_1\gamma_2$ were performed as described previously (Schneider and Seifert, 2009). All experimental data were analyzed with the software Prism 5.0 (GraphPad Software Inc., San Diego, CA). Statistical comparisons of the data shown in Fig. 4 were performed with Prism 5.0 as well. In some control experiments, we analyzed membranes expressing only $G\alpha_{i2}$ and $G\beta_1\gamma_2$ without hH_4R. Asthma data are the means ± S.D. of six to eight animals per group. Data shown for recombinant hH_4R are the means ± S.E.M. of at least three independent experiments.

Construction of an Inactive and Active hH_4R Model with Suprahistaprodifen in the Binding Pocket. For generation of an inactive hH_4R model, the sequence of hH_4R was aligned to hβ_2AR (Ballesteros et al., 2001). Based on this alignment, the homology model of the inactive hH_4R was generated using the crystal structure of the hβ_2AR (Protein Data Bank code 2rh1) (Cherezov et al., 2007; Rasmussen et al., 2007; Rosenbaum et al., 2007). The software package SYBYL 7.3 (Tripos, St. Louis, MO) was used. Loops with different length compared with the hβ_2AR were modeled using the Loop Search module of SYBYL 7.3. Because of the lack of sufficient experimental data concerning the structure of the I3-loop and parts of the C terminus, both were included only partially in the modeling studies. This approximation should not have much influence to the modeling of the binding-mode of the ligand. Subsequently, the receptor

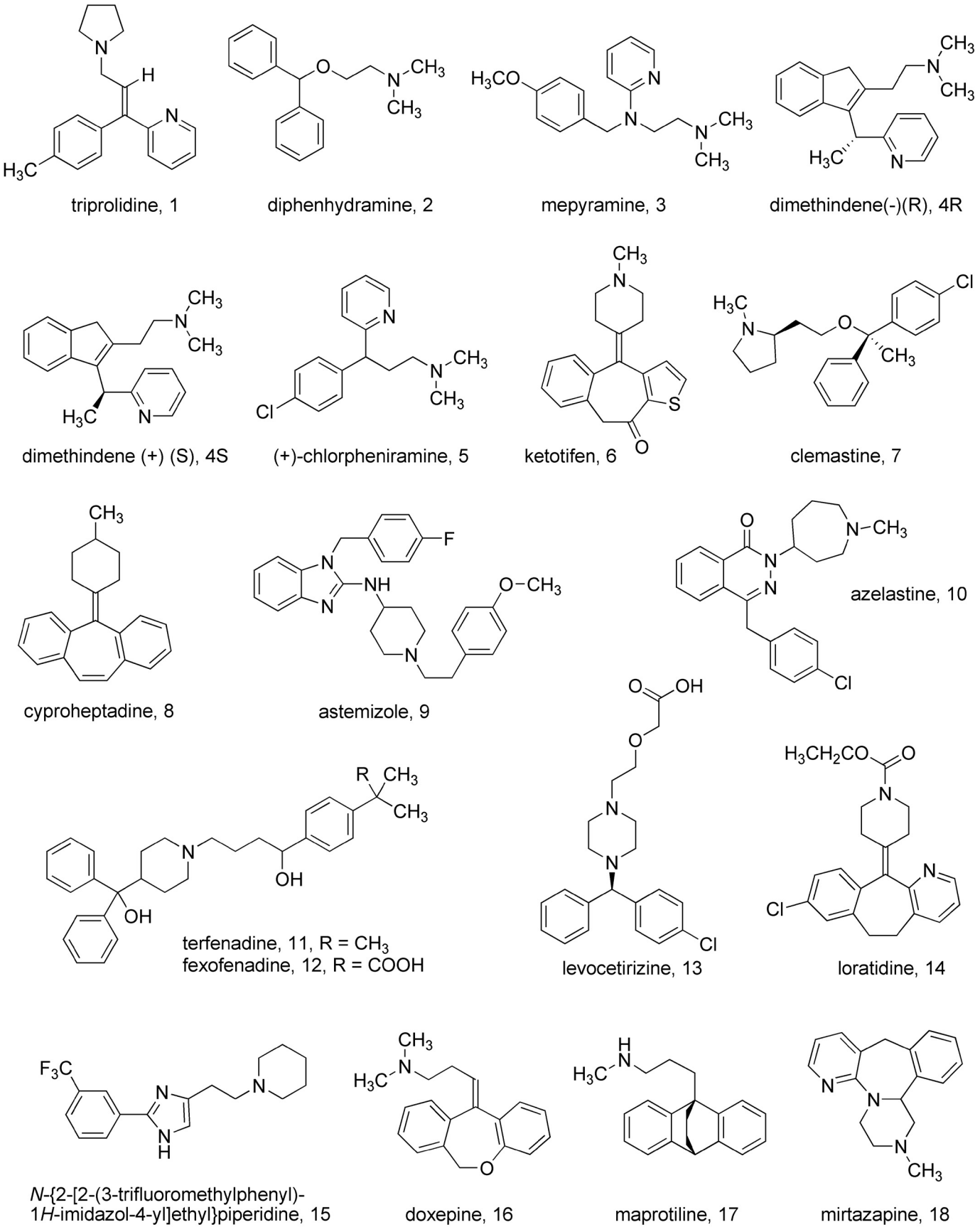

Fig. 1. Structures of H_1R antagonists. First generation H_1R antagonists (**1-8**), second generation H_1R antagonists (**9-14**), and miscellaneous H_1R antagonists (**15-18**).

was minimized carefully. Thereafter, the receptor was manually placed in a 1-palmitoyl-2-oleoyl-*sn*-glycero-3-phosphocholine membrane bilayer (104 molecules), and suprahistaprodifen was positioned manually into the proposed binding-pocket in two different orientations. With GROMACS 3.3.1 (http://www.gromacs.org/), a simulation box containing intra- and extracellular water (12,759 molecules) was constructed. Because of the positively charged receptor and ligand, electroneutrality was achieved by placing 6 sodium and 14 chloride ions inside the box. The whole system was minimized with GROMACS 3.3.1. To refine the hH_4R homology model, representing the inactive state, distance-restrained molecular dynamic simulations using the constraints of the inactive conformation (Niv et al., 2006) were also performed. The active model of the hH_4R was generated with a distance-restrained MD simulation, based on the constraints for the active conformation (Niv et al., 2006). We used the same constraints as already described for the corresponding gpH_1R amino acids (Strasser et al., 2008a). In addition, we applied distance restraints for the hydrogen-bonds of the transmembrane helices (Strasser and Wittmann, 2007). All simulations were carried out as described for H_1R (Strasser et al., 2008a). For all molecular dynamics simulations, we used the software package GROMACS 3.3.1 with the ffG53A6 force field (Oostenbrink et al., 2004). The force field parameters for suprahistaprodifen were adopted from the ffG53A6 force field. To assess the influence of the $Tyr^{2.61}Asn$ mutation in hH_4R (Fig. 3) on interaction with suprahistaprodifen, the corresponding mutants were generated for the inactive and active hH_4R. Subsequently, suprahistaprodifen was docked in both orientations and MD simulations were performed as described for the wild-type hH_4R.

Results

Effect of Mepyramine and JNJ 7777120 in an Acute Murine Asthma Model. Asthma in mice was induced by

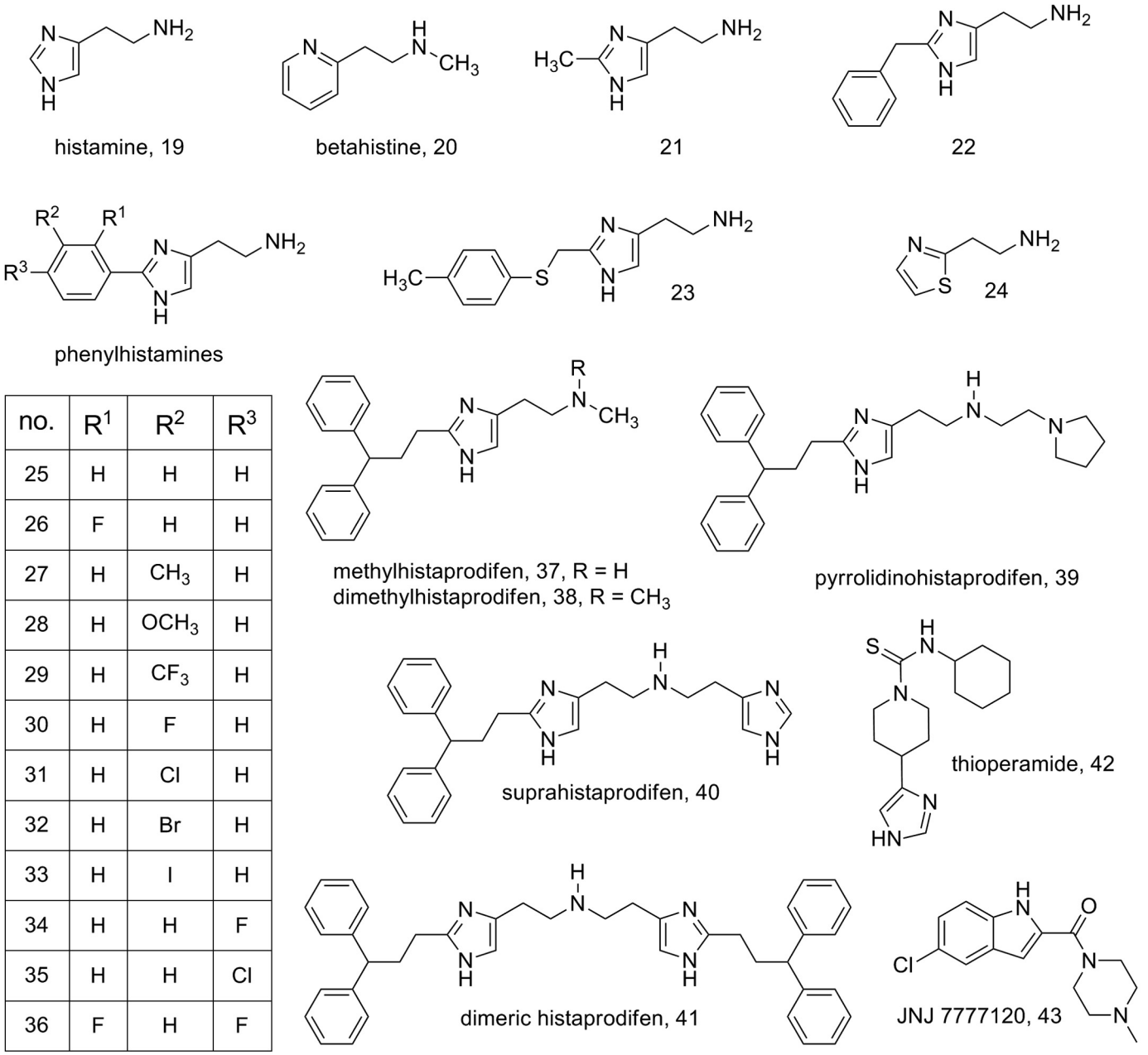

no.	R^1	R^2	R^3
25	H	H	H
26	F	H	H
27	H	CH_3	H
28	H	OCH_3	H
29	H	CF_3	H
30	H	F	H
31	H	Cl	H
32	H	Br	H
33	H	I	H
34	H	H	F
35	H	H	Cl
36	F	H	F

Fig. 2. Structures of H_1R agonists, thioperamide, and JNJ 7777120. Histamine (**19**), small agonists (**20-24**), phenylhistamines (**25-36**), histaprodifens (**37-41**), and thioperamide (**42**).

two intraperitoneal injections of ovalbumin/aluminum hydroxide on days 1 and 14, followed by four inhalation challenges with ovalbumin aerosol on days 21 to 24. On day 25 of the protocol, animals were sacrificed, and eosinophils were counted on cytospin preparations of bronchoalveolar lavage fluid. This sensitization/challenge protocol resulted in a massive eosinophilia in mice (Fig. 4). In accordance with Dunford et al. (2006), the H_4R antagonist JNJ 7777120 applied during the sensitization phase moderately diminished eosinophilia (30.9% reduction). However, this effect did not reach statistical significance. The H_1R antagonist mepyramine exhibited only a minimal inhibitory effect on eosinophilia (8.7% reduction, not significant). When combined, however, JNJ 7777120 and mepyramine showed a strikingly synergistic inhibitory effect on eosinophilia (64.8% reduction, $p < 0.05$) compared with the control. Compared with mepyramine alone, the combination of both drugs reduced eosinophilia by 61.5% ($p < 0.05$). These data show that both the H_1R and H_4R play a role in the pathogenesis of acute bronchial asthma (in this murine model, at least) and support the notion that the development of dual H_1R/H_4R antagonists constitutes an important goal (Thurmond et al., 2008). Furthermore, the animal studies provided the rationale for our studies assessing the effects of known H_1R agonists and H_1R antagonists on hH_4R, constituting the basis for the long-term goal of developing potent dual H_1R/H_4R antagonists.

Use of the hH_4R-RGS19 Fusion Protein as Model System for the Analysis of H_1R Ligands. In analogy to other G_i-coupled receptors (Seifert and Wenzel-Seifert, 2002), we coexpressed hH_4R with $G\alpha_{i2}$ and $G\beta_1\gamma_2$ in Sf9 insect cells to reconstitute high-affinity [^{3}H]histamine binding and GTPase activity (Schneider et al., 2009). This coexpression system

```
                |-----------N-Terminus--------||-------------TM1------------||-I1-||--------TM2------
hH1R      1--------MSLPNSSCLLEDKMCEGNKTTMASPQLMPLVVVLSTICLVTVGLNLLVLYAVRSERKLHTVGNLYIVSLSVADLIVGA-78
hH4R      1--------------------MPDTNSTINLSLSTRVTLAFFMSLVAFAIMLGNALVILAFVVDKNLRHRSSYFFLNLAISDFFVGV-66

                -----------||-E1-||--------------TM3--------------||----I2-----||---------TM4--------
hH1R     79-VVMPMNILYLLMSKWSLGRPLCLFWLSMDYVASTASIFSVFILCIDRYRSVQQPLRYLKYRTK-TRASATILGAWFLSFLWVIPI-162
hH4R     67-ISIPLYIPHTLFE-WDFGKEICVFWLTTDYLLCTASVYNIVLISYDRYLSVSNAVSYRTQHTGVLKIVTLMVAVWVLAFLVNGPM-150

                -||---------E2---------||----------TM5-----------||------------I3---------||---------
hH1R     163-LGWNHFMQQTSVRREDKCETDFYDVTWFKVMTAIINFYLPTLLMLWFYAKIYKAVRQHCQ.....QYVSGLHMNRERKAAKQLGF-419
hH4R     151-ILV-SESWKDEG--SE-CEPGFFSEWYILAITSFLEFVIPVILVAYFNMNIYWSLWKRDH.....HQREHVELLRARRLAKSLAI-307

                -------TM6----------||---E3--||--------TM7--------||----------C-Terminus----------|
hH1R     420-IMAAFILCWIPYFIFFMVIAFCKNC--CNEHLHMFTIWLGYINSTLNPLIYPLCNENFKKTFKRILHIRS--------------487
hH4R     308-LLGVFAVCWAPYSLFTIVLSFYSSATGPKSVWYRIAFWLQWFNSFVNPLLYPLCHKRFQKAFLKIFCIKKQPLPSQHSRSVSS-390
```

Fig. 3. Alignment of the amino acid sequences of hH_1R and hH_4R. Dots in the sequences of hH_1R and hH_4R indicate incomplete amino acid sequence of the long intracellular loop I3. Hyphens indicate missing amino acids. Amino acids with gray shading are the most conserved amino acids (X.50, X being the number of the TM domain), according to the numbering scheme used by Ballesteros et al. (2001). Amino acids in white with black shading indicate the amino acids that are proposed to interact with the dimeric histaprodifen in the binding pocket of hH_1R (Strasser et al., 2008b) or hH_4R (this study) based on molecular dynamics simulations. The amino acid sequences are given in the one-letter code, and the alignment was performed manually.

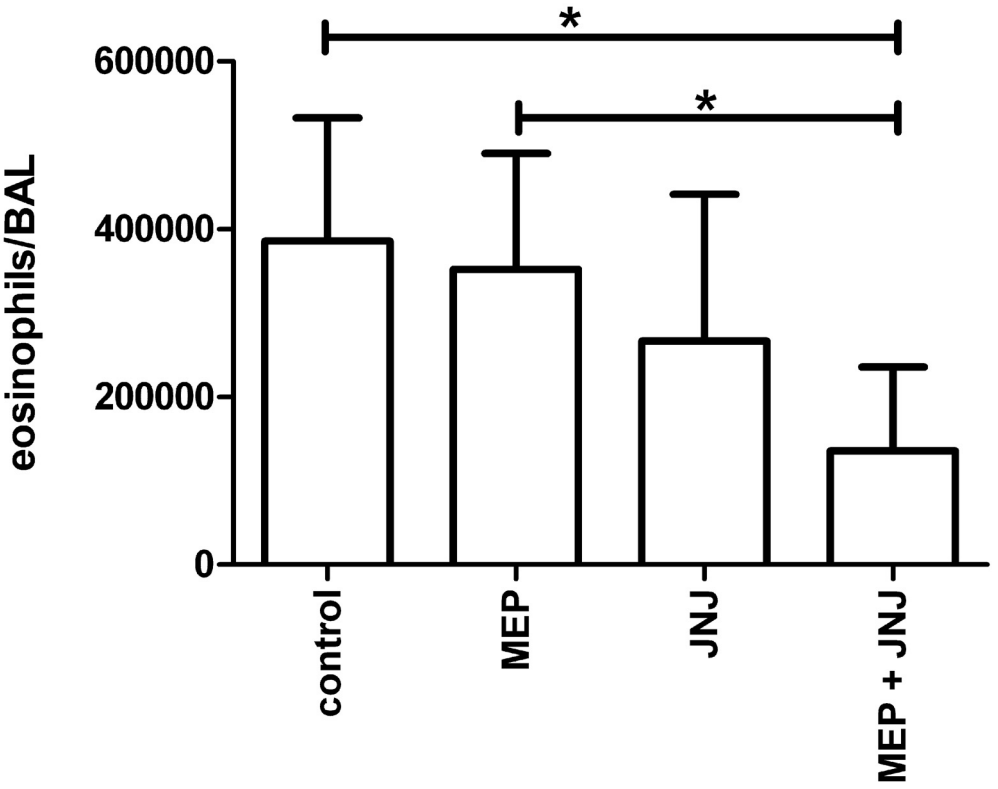

Fig. 4. Effects of mepyramine and JNJ 7777120 on eosinophil accumulation in the bronchoalveolar lavage fluid in an acute murine asthma model. In BALB/c mice, acute ovalbumin-induced asthma was induced as described under *Materials and Methods*. Mice were injected s.c. with solvent (100 μl of DMSO, control), 20 mg/kg mepyramine (MEP), 20 mg/kg JNJ 7777120 (JNJ), or a combination of 20 mg/kg mepyramine plus 20 mg/kg JNJ 7777120 30 min before and 2 h after the sensitization with ovalbumin at days 1 and 14. At days 21 to 24 animals were challenged with ovalbumin, and at day 25, eosinophils were counted in the bronchoalveolar lavage fluid. Data are expressed as absolute numbers of eosinophils per bronchoalveolar lavage (BAL) fluid of individual animals. The effects of antagonists on eosinophilia were compared with each other and the control group using one-way analysis of variance, Bartlett's test for equal variances and Bonferroni's multiple comparison test. Data shown are the means ± S.D. of six animals in the control group and eight animals in the drug groups. One-was analysis of variance, $p < 0.0107$ (not shown in table). Bartlett's test for equal variances, $p < 0.57$ (not significant, not shown in table). *, $p > 0.05$ in Bonferroni's multiple comparison test. The other comparisons were not statistically significant.

was functional, but the signals in the GTPase assay were relatively small. Therefore, for more detailed pharmacological studies, we aimed at developing a system that yielded a better signal-to noise ratio. As a result of this effort, we established a coexpression system of the hH_4R-RGS19 fusion protein with $G\alpha_{i2}$ and $G\beta_1\gamma_2$ in Sf9 insect cells (Schneider and Seifert, 2009). Previous studies with hH_1R showed that RGS proteins enhance signals in the GTPase assay (Seifert et al., 2003). In fact, the RGS19 protein also substantially enhanced the signals in the GTPase assay for hH_4R without changing the pharmacological profile of hH_4R (Schneider and Seifert, 2009). Enhanced signals in the GTPase assay are particularly important for the quantitative assessment of the potencies and efficacies of partial agonists and partial inverse agonists (Seifert et al., 2003; Schneider and Seifert, 2009). Moreover, in the expression system used, G-protein availability is not a limiting factor because the $G\alpha_{i2}$ expression level is about 200-fold higher than the hH_4R-RGS19 expression level (~300 versus ~1.5 pmol/mg) (Schneider and Seifert, 2009; Schneider et al., 2009). Accordingly, we used the hH_4R-RGS19 fusion protein as system to assess the interaction of H_1R ligands with hH_4R. The pharmacological properties of hH_1R were also assessed in the GTPase assay using RGS4 or RGS19 as signal enhancer (Seifert et al., 2003). Thus, another important advantage of the GTPase assay compared with other assays is the fact that it represents a proximal measure of GPCR/ligand interaction and allows direct comparison of hH_1R and hH_4R (Seifert et al., 2003; Igel et al., 2009).

Analysis of H_1R Antagonists and H_1R Agonists at hH_4R in the Competition Binding Assay. The affinities of H_1R antagonists and agonists, determined at hH_4R in the [^{3}H]histamine competition binding assay, are summarized in Table 1. Figure 5A shows representative competition binding isotherms for selected ligands. All binding isotherms were monophasic with a Hill slope close to unity, indicative for a single ligand binding site. First-generation H_1R antagonists **1** to **8** bound to hH_4R with pK_i values in the ~4.0 to 5.0 range. For comparison, H_1R antagonists bind to hH_1R with functional pK_b values (inhibition of histamine-stimulated GTP hydrolysis) in the ~8.0 to 9.0 range (Seifert et al., 2003); i.e., the compounds exhibit a strong preference for hH_1R compared with hH_4R. The second-generation H_1R antagonists **9** to **14** exhibited pK_i values at hH_4R of ~5.0, whereas the corresponding pK_b values at hH_1R are in the ~7.0 to 9.0 range (Seifert et al., 2003). Likewise, the antidepressants **16** to **18** were only low-affinity hH_4R ligands.

In radioligand binding studies, histamine possesses an approximate 100-fold higher affinity for hH_4R than for hH_1R (Table 1) (Seifert et al., 2003; Strasser et al., 2008a). At hH_1R, phenylhistamines exhibit pK_i values of ~6.0 (Seifert et al., 2003), whereas at hH_4R, the pK_i values of phenylhistamines **24** to **36** range between ~5.0 and 6.0 (Table 1); i.e., the affinities of phenylhistamines at hH_4R approach the affinities of hH_1R within 1 order of magnitude (Seifert et al., 2003). Histaprodifens **37**, **38**, and **41** bind to hH_1R with pK_i values of ~6.5 (Seifert et al., 2003; Strasser et al., 2008), whereas at hH_4R, the corresponding pK_i values of histaprodifens **37**, **38**, and **41** range between ~4.0 and 5.5 (Table 1). It is noteworthy that histaprodifen **40** (suprahistaprodifen) exhibits almost identical affinity at hH_1R (pK_i, 5.76; Strasser et al., 2008a) and hH_4R (pK_i 5.77; Table 1) in the competition binding assay.

Analysis of H_1R Antagonists and H_1R Agonists at hH_4R in the Steady-State GTPase Assay. The potencies and (inverse) agonist efficacies of H_1R agonists and antagonists at hH_4R, determined in the steady-state GTPase assay, are summarized in Table 1 as well, and Fig. 5B shows concentration-response curves for selected compounds in the GTPase assay. Triprolidine (**1**) was an inverse agonist at hH_4R with low potency. In contrast, diphenhydramine (**2**) showed a neutral antagonistic effect at hH_4R. For mepyramine (**3**) an inverse agonistic effect was observed at hH_4R with a potency in the same range as for triprolidine (**1**). Dimethindene (**4R** and **4S**) showed inverse agonistic effect at hH_4R and exhibited moderate potency. Potencies and E_{max} values of chlorpheniramine (**5**) and ketotifen (**6**) were in the same range at hH_4R. Both compounds exhibited low potency and were inverse agonists. The potency of clemastine (**7**) was in the same range as for chlorpheniramine (**5**) or ketotifen (**6**), but the efficacy was significantly decreased. In contrast, cyproheptadine (**8**) acted as neutral antagonist at hH_4R. Astemizole (**9**) showed a large inverse agonistic effect, but a rather low potency.

For azelastine (**10**), the potency and efficacy were in the same range as for ketotifen (**6**). Terfenadine (**11**) acted as partial agonist at hH_4R, whereas fexofenadine (**12**) showed an inverse agonist effect. Levocetirizine (**13**) and loratadine (**14**) exhibited a weak partial agonistic effect, whereas compound **15** showed inverse agonism and low potency. Doxepine (**16**) and mirtazapine (**18**) were inverse agonists at hH_4R. In contrast, maprotiline (**17**) acted as neutral antagonist. Compared with hH_4R, hH_1R possesses only low constitutive activity and accordingly, first- and second-generation H_1R antagonists exhibit only minimal inverse agonistic efficacies (Seifert et al., 2003).

The highest potency among all analyzed compounds studied at hH_4R was found for histamine (**19**). Betahistine (**20**) exhibited partial agonism at hH_4R but with a much lower potency than at hH_1R (Seifert et al., 2003). 2-Methylhistamine (**21**) exhibited high efficacy, but compared with histamine (**19**), the potency was decreased by more than 100-fold (Fig. 5). At hH_1R, 2-methylhistamine (**21**) is just 4-fold less potent than histamine (Seifert et al., 2003). 2-Benzylhistamine (**22**) showed weak partial agonism at hH_4R. At hH_1R, benzylhistamine (**22**) is a moderately strong partial agonist (Seifert et al., 2003). The efficacy of compound **23** was significantly increased compared with **22**, but **23** exhibited a rather low potency. Compared with histamine (**19**), only weak partial agonism with a potency <4 was observed for thiazolylethanamine (**24**). At hH_1R, thiazolylethanamine (**24**) has potency and efficacy similar to that of histamine (**19**) (Seifert et al., 2003).

The unsubstituted phenylhistamine (**25**) was a weak partial hH_4R agonist with a low potency. The introduction of a fluoro moiety in *ortho* position (**26**) decreased potency but increased efficacy. The methyl moiety or methoxy moiety in compound (**27**) and (**28**) showed no large influence onto the efficacy compared with the unsubstituted phenylhistamine (**25**), but the potency was significantly decreased. In contrast, the trifluoromethyl moiety in *meta* position (**29**) increased potency as well as efficacy compared with the unsubstituted phenylhistamine (**25**). The potencies of halogen *meta*-substi-

tuted phenylhistamines increased potency in the series fluorine (**30**) < bromine (**32**) < chlorine (**31**) < iodine (**33**) and increased efficacy in the series iodine (**33**) < chlorine (**31**) < fluorine (**30**) < bromine (**32**). The fluoro moiety in *para* substitution (**34**) exhibited no influence on efficacy compared with the unsubstituted phenylhistamine (**25**), but the potency was significantly decreased. In contrast, the chloro substitution in the same position decreased efficacy (**35**). For the phenylhistamine derivative with a fluoro substitution in *ortho* and *para* position (**36**), the potency was significantly increased compared with the mono-substituted derivatives **26** and **34**, but the efficacy was in the same range as for the *ortho*-substituted derivative **26**. The structure-activity relationships of 2-phenylhistamines at hH_4R and hH_1R are different. In general, the potencies of 2-phenylhistamines at hH_1R are about 1 order of magnitude higher than at hH_4R. Moreover, the compounds differ from each other at both receptors in terms of efficacy. In general, efficacies of 2-phenylhistamines are lower at hH_4R than at hH_1R (Table 1) (Seifert et al., 2003). As a striking example, phenylhistamine (**35**) exhibited a 4-fold higher efficacy at hH_1R than at hH_4R.

The potency of methylhistaprodifen (**37**) at hH_4R was in the same range as for phenylhistamine (**25**), but in contrast to phenylhistamine (**25**), methylhistaprodifen (**37**) showed inverse agonism. The potency of dimethylhistaprodifen (**38**) at hH_4R was decreased compared with methylhistaprodifen (**37**), and the inverse agonistic effect of (**38**) (Fig. 5) was not as large as for (**37**). Pyrrolidinohistaprodifen (**39**) showed a potency <4, but the efficacy was in the same range as for dimethylhistaprodifen (**38**). Compared with methylhistaprodifen (**37**), the potency of suprahistaprodifen (**40**) was increased, and in contrast to the histaprodifen derivatives **37** to

TABLE 1

Affinities of H_1R antagonists and agonists at hH_4R-RGS19 coexpressed with $G\alpha_{i2}$ and $G\beta_1\gamma_2$ in Sf9 cell membranes determined in the equilibrium competition binding assay and potencies and efficacies of H_1R ligands in the steady-state GTPase assay

Competition binding with Sf9 membranes coexpressing hH_4R-RGS19 with $G\alpha_{i2}$ and $G\beta_1\gamma_2$ was performed as described under *Materials and Methods*. Data were analyzed by nonlinear regression and were best fit to one-site (monophasic) competition curves with a Hill slope close to unity. Data shown are the means ± S.E.M. of at least three experiments with independent membrane preparations in duplicates each. All GTPase experiments were performed as described under *Materials and Methods*. Data were analyzed by nonlinear regression and were best fit to sigmoidal concentration-response curves. The efficacy (E_{max}) of histamine was set 1.00 and the efficacy of thioperamide was set to −1.00. The E_{max} values of all other agonists and partial agonists were referred to histamine, whereas the E_{max} values of all other inverse agonists were referred to thioperamide. Data shown are means ± S.E.M. of at least three experiments performed in duplicates or triplicates each. Membranes were used from independent membrane preparations.

	Compound	hH_4R		
		pK_i	pEC_{50}	E_{max}
H_1R antagonists				
First generation	**1**	4.06 ± 0.01	4.96 ± 0.07	−0.34 ± 0.01
	2	4.37 ± 0.10	N.D.	0.05 ± 0.01
	3	<4	5.17 ± 0.01	−0.21 ± 0.03
	4R	<4	4.65 ± 0.07	−0.21 ± 0.03
	4S	<4	4.43 ± 0.02	−0.21 ± 0.03
	5	4.56 ± 0.01	4.60 ± 0.09	−0.34 ± 0.04
	6	4.30 ± 0.11	4.59 ± 0.05	−0.30 ± 0.03
	7	4.80 ± 0.07	4.68 ± 0.08	−0.62 ± 0.06
	8	4.79 ± 0.09	N.D.	−0.04 ± 0.06
Second generation	**9**	5.10 ± 0.06	<4	−0.92 ± 0.06
	10	4.30 ± 0.03	4.43 ± 0.06	−0.37 ± 0.04
	11	4.83 ± 0.16	N.D.	0.16 ± 0.02
	12	<4	N.D.	−0.13 ± 0.01
	13	<4	N.D.	0.13 ± 0.01
	14	4.74 ± 0.02	N.D.	0.06 ± 0.02
	15	4.20 ± 0.09	4.58 ± 0.04	−0.37 ± 0.02
Antidepressants	**16**	4.78 ± 0.10	N.D.	−0.15 ± 0.05
	17	4.48 ± 0.03	N.D.	0.01 ± 0.06
	18	<4	N.D.	−0.10 ± 0.08
Histamine	**19**	8.07 ± 0.14	7.93 ± 0.06	1.00
Betahistine	**20**	4.09 ± 0.07	<4	0.37 ± 0.02
2-Methylhistamine	**21**	6.05 ± 0.01	5.42 ± 0.13	0.85 ± 0.01
2-Benzylhistamine	**22**	4.83 ± 0.01	N.D.	0.14 ± 0.01
	23	4.74 ± 0.05	4.59 ± 0.13	0.54 ± 0.01
	24	<4	<4	0.22 ± 0.02
2-Phenylhistamines	**25**	4.79 ± 0.04	4.92 ± 0.07	0.32 ± 0.02
	26	4.86 ± 0.13	4.01 ± 0.08	0.62 ± 0.04
	27	5.18 ± 0.19	<4	0.33 ± 0.02
	28	4.75 ± 0.15	<4	0.20 ± 0.01
	29	5.91 ± 0.12	5.83 ± 0.08	0.51 ± 0.02
	30	5.19 ± 0.14	4.76 ± 0.03	0.53 ± 0.02
	31	5.51 ± 0.04	5.40 ± 0.08	0.44 ± 0.02
	32	5.76 ± 0.01	5.02 ± 0.03	0.61 ± 0.02
	33	5.54 ± 0.07	5.86 ± 0.08	0.30 ± 0.02
	34	5.26 ± 0.07	<4	0.39 ± 0.01
	35	4.76 ± 0.09	N.D.	0.13 ± 0.01
	36	5.76 ± 0.05	5.04 ± 0.07	0.65 ± 0.02
Histaprodifens	**37**	5.17 ± 0.05	5.20 ± 0.11	−0.93 ± 0.03
	38	4.23 ± 0.04	4.47 ± 0.16	−0.62 ± 0.03
	39	4.18 ± 0.01	<4	−0.62 ± 0.03
	40	5.77 ± 0.05	5.82 ± 0.12	0.25 ± 0.02
	41	5.57 ± 0.08	4.81 ± 0.01	−1.27 ± 0.02

N.D., not determined.

39, suprahistaprodifen (**40**) exhibited partial agonism. The potency of dimeric histaprodifen (**41**) compared with suprahistaprodifen (**40**) was significantly decreased. Dimeric histaprodifen (**41**) acted as an inverse agonist, like histaprodifen derivatives **37** to **39**, but compared with these derivatives, the inverse agonism was more remarkable (Fig. 5). In addition, the efficacy of dimeric histaprodifen (**41**) was more negative than for thioperamide (**42**), but the potency of **41** compared with **42** was significantly decreased. The inverse agonistic effect of histaprodifen (**41**) was mediated via hH_4R and not an unspecific effect, because in membranes expressing only $G\alpha_{i2}\beta_1\gamma_2$, the compound was without effect on GTPase activity (data not shown). The structure-activity relationships of histaprodifens at hH_1R and hH_4R are different. In particular, all compounds studied are partial hH_1R agonists with no inverse agonistic activity (Seifert et al., 2003; Strasser et al., 2008a). Moreover, histaprodifens are generally at least 10-fold more potent at hH_1R than at hH_4R.

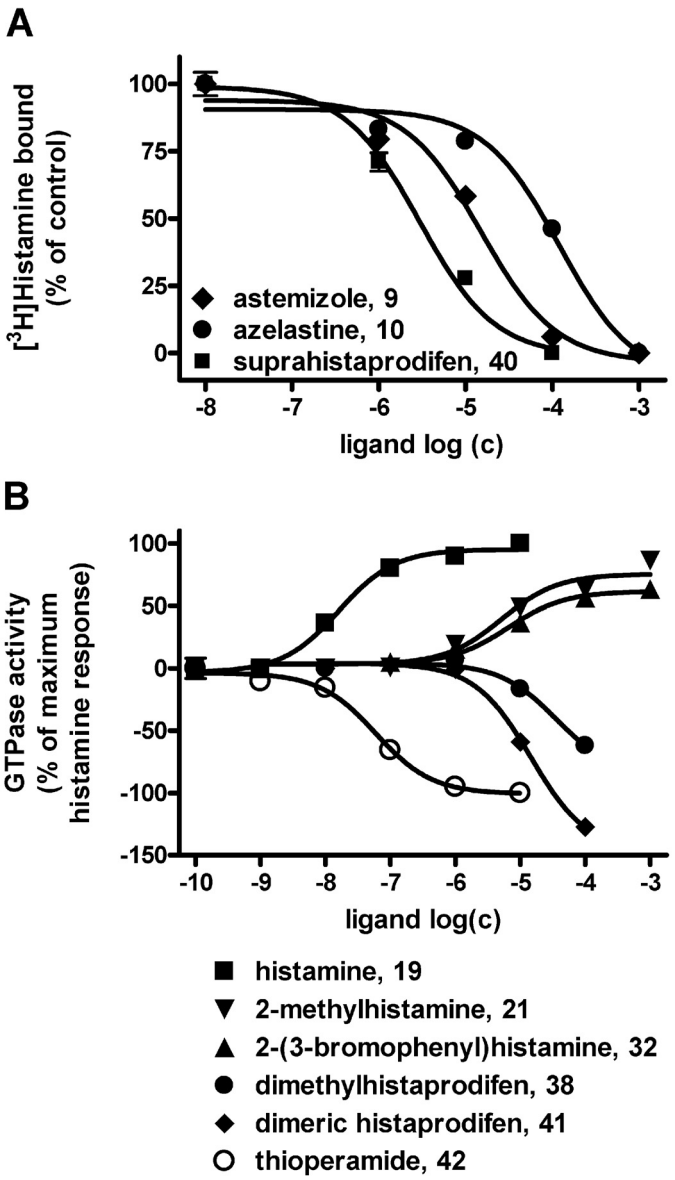

Fig. 5. Competition binding isotherms for selected compounds at hH_4R-RGS19 coexpressed with $G\alpha_{i2}$ and $G\beta_1\gamma_2$ and concentration-response curves for selected compounds at hH_4R-RGS19 in the steady-state GTPase assay. A, the competition binding experiments were performed using Sf9 cell membranes coexpressing hH_4R-RGS19, $G\alpha_{i2}$, and $G\beta_1\gamma_2$ in presence of 10 nM [^{3}H]histamine as described under *Materials and Methods*. Data were analyzed by nonlinear regression and were best fit to one-site (monophasic) competition curves. Data shown are the means ± S.E.M. of at least three experiments in duplicates each. Membranes were used from independent membrane preparations. B, the GTPase experiments were performed using Sf9 cell membranes coexpressing hH_4R-RGS19, $G\alpha_{i2}$, and $G\beta_1\gamma_2$ as described under *Materials and Methods*. Data shown are the means ± S.E.M. of at least three experiments in duplicate, each with independent membrane preparations.

Binding Modes of Histraprodifens at the hH_4R. Dimeric histaprodifen (**41**) is a large bivalent ligand with numerous functional groups (Fig. 2). The distance between the two imidazole groups in dimeric histaprodifen ranges between 7.5 and 11.5 Å, depending on the actual ligand conformation. Thus, the question arises whether dimeric histaprodifen could bind to the ligand binding sites in two adjacent hH_4R molecules (i.e., hH_4R dimers), as was proposed for other ligand/GPCR pairs (Lezoualc'h et al., 2009). However, the distance of the two $Asp^{3.50}$ positions in a hH_4R dimer would amount to 30 to 35 Å (Rasmussen et al., 2007; Rosenbaum et al., 2007) (i.e., a distance far longer than the distance between the two imidazole groups). Moreover, in case of a ligand bridging two receptor molecules, the linker between functional groups would have to be much longer than 30 to 35 Å, because the two Asp residues cannot be directly bridged through the transmembrane domains but would have to use the route via the extracellular domains (Lezoualc'h et al., 2009). Finally, studies with hH_1R have clearly shown that dimeric histaprodifen interacts with a single hH_1R molecule (Strasser et al., 2008a, 2009). Accordingly, it is very likely that dimeric histaprodifen also binds to a single hH_4R molecule.

The data obtained in the steady-state GTPase assays show that histaprodifens act as inverse agonists at hH_4R, except for suprahistaprodifen (**40**), which shows partial agonistic effects. Based on the symmetrical structure of dimeric histaprodifen and partially symmetrical structure of suprahistaprodifen, it can be proposed that suprahistaprodifen can bind to hH_4R in two different orientations as already described for the H_1R (Strasser et al., 2008a). Because the diphenylpropyl moiety of all analyzed histaprodifen derivatives, except for suprahistaprodifen, is located in a binding-pocket near transmembrane helix (TM) 5, the diphenylpropyl moiety located in this pocket (Fig. 6) may be responsible for the inverse agonistic effect as a result of stabilization of the inactive state of the hH_4R. Thus, suprahistaprodifen, showing partial agonistic effects, binds to hH_4R only in orientation 2, or binds to hH_4R in orientations 1 and 2, orientation 2 showing a higher agonistic effect than orientation 1 showing an inverse agonistic effect.

Based on this hypothesis, we analyzed the binding of suprahistaprodifen in orientation 1 in the inactive state and the binding of suprahistaprodifen in orientation 2 in the active state of the hH_4R. We found that for orientation 1 (Fig. 6A), the diphenylpropyl moiety of suprahistaprodifen is located deeply in a pocket between TM3, TM5, and TM6. One phenyl group of the diphenylpropyl moiety establishes an aromatic interaction with $Trp^{6.48}$ in the inactive conformation. Thus, $Trp^{6.48}$, a crucial amino acid of the highly conserved toggle switch (Crocker et al., 2006) is not able to move into its active conformation. $Phe^{5.47}$ and $Phe^{6.44}$ are located near to the diphenylpropyl moiety and

partially build the hydrophobic pocket. The nonterminal imidazole moiety establishes a stable hydrogen-bond to $Glu^{5.46}$, and sometimes a hydrogen-bond to $Tyr^{6.51}$ was observed. The positively charged amino group interacts with the highly conserved $Asp^{3.32}$. An analogous ligand-$Asp^{3.32}$ interaction was also described for other ligands (Jójárt et al., 2008). At H_1R, the corresponding imidazole moiety establishes a hydrogen bond to $Ser^{3.36}$ (Strasser et al., 2008a). At hH_4R, at the corresponding position, there is not a serine but a cysteine. We did not observe a hydrogen-bond between the imidazole moiety and $Cys^{3.36}$, in contrast to the observations made for H_1R and the corresponding $Ser^{3.36}$. The reason for this may be the reduced flexibility of this imidazole moiety as a result of the hydrogen bond to $Glu^{5.46}$, resulting in a horizontal conformation of the imidazole moiety at hH_4R, in contrast to the vertical conformation at H_1R. The terminal imidazole moiety is located in a pocket built by $Tyr^{2.61}$, $Trp^{3.28}$, and $Trp^{7.40}$ and showed a high flexibility during the simulation. In addition, a stable hydrogen-bond between $Tyr^{2.61}$ and $Asp^{3.32}$ was observed during the entire simulation.

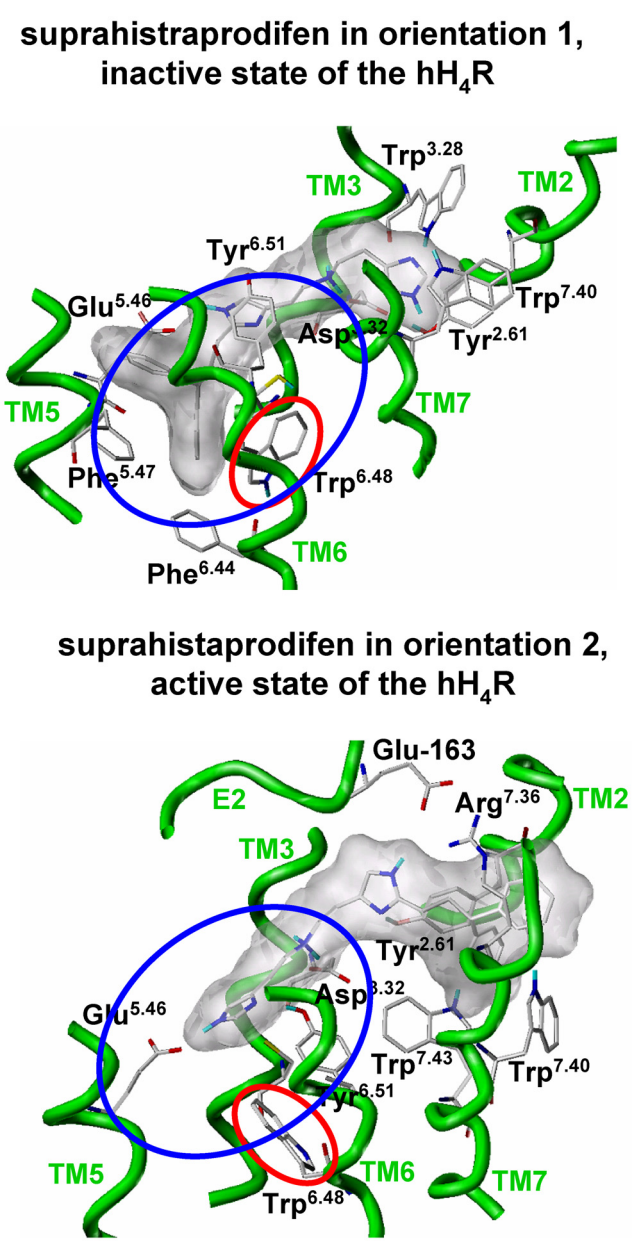

Fig. 6. Binding mode of suprahistaprodifen 40 in the inactive and active hH_4R model. A, snapshot of suprahistaprodifen (**40**) in the binding pocket of the inactive state of the hH_4R during MD simulation. B, snapshot of suprahistaprodifen (**40**) in the binding pocket of the active state of the hH_4R during MD simulation. The models based on the crystal structure of the $h\beta_2AR$ were generated as described under *Materials and Methods*. The MD simulations were performed as described under *Materials and Methods*. The blue circle indicates the histaprodifen binding-pocket, and the red circle indicates the highly conserved $Trp^{6.48}$, which is involved in the rotamer toggle switch during receptor activation.

In orientation 2 (Fig. 6B) the diphenylpropyl moiety of the suprahistaprodifen is located in a hydrophobic pocket, including the amino acids $Tyr^{2.61}$, $Trp^{7.43}$, and $Trp^{7.40}$. For the nonterminal imidazole moiety, no stable and distinct hydrogen bonds were observed. The positively charged amino group interacts electrostatically with $Asp^{3.32}$. The terminal imidazole moiety establishes a hydrogen bond to $Glu^{5.46}$, analogous to the binding-mode of histamine itself at the hH_4R (Jongejan et al., 2008). In addition, hydrogen-bonds between $Tyr^{6.51}$ and the terminal imidazole moiety were observed. Besides that, the molecular dynamics simulations revealed a stable electrostatic interaction between Glu-163 (E2-loop) and $Arg^{7.36}$. This interaction is located above the bound ligand and thus closes the entry to the binding pocket. In orientation 1 of suprahistaprodifen in the inactive hH_4R, a stable hydrogen bond between $Asp^{3.32}$ and $Tyr^{2.61}$ was found, but this interaction was not observed for orientation 2 in the active conformation of the hH_4R.

In hH_1R, $Asn^{2.61}$ has been proposed to interact with histaprodifens (Bruysters et al., 2005; Strasser et al., 2008b). Because this amino acid is not conserved in hH_4R ($Tyr^{2.61}$) (Fig. 3), the question arises of whether this amino acid contributes to the differential interaction of suprahistaprodifen with hH_1R and hH_4R. However, the simulation of the $Tyr^{2.61}$Asn mutant hH_4R with the suprahistaprodifen in its inactive conformation (orientation 1) revealed no influence on the binding-mode of suprahistaprodifen. The terminal imidazole moiety is located in a pocket, built by $Asn^{2.61}$, $Trp^{3.28}$, and $Trp^{7.40}$ and showed high flexibility during the simulation, as already observed for wild-type hH_4R. In addition, a stable hydrogen-bond between $Asn^{2.61}$ and $Trp^{3.28}$ was observed during the entire simulation. Thus, the exchange of $Tyr^{2.61}$ into $Asn^{2.61}$ in hH_4R is suggested to change the hydrogen bond network in the binding-pocket of the receptor but has no influence onto binding of suprahistaprodifen in orientation 1.

In the $Tyr^{2.61}$Asn mutant of hH_4R in its active conformation, with suprahistaprodifen bound in orientation 2, a stable hydrogen bond between $Asn^{2.61}$ and $Trp^{3.28}$ was observed during the simulation. No hydrogen bond interaction between $Asn^{2.61}$ and suprahistaprodifen was observed. However, because of the lack of the aromatic ring of $Tyr^{2.61}$ in the mutant hH_4R, the MD simulations revealed a slight conformational change of the diphenylpropyl moiety of suprahistaprodifen (orientation 2). Thus, overall, there is no evidence that the exchange of $Asn^{2.61}$ against $Tyr^{2.61}$ in hH_4R compared with hH_1R has a major impact on interaction with suprahistaprodifen. Accordingly, we did not proceed to generate the actual $Tyr^{2.61}$Asn mutant hH_4R and analyze it in binding and GTPase experiments.

Discussion

Both the H_1R and H_4R have been proposed to be involved in the pathogenesis of bronchial asthma, giving rise to the hypothesis that dual H_1R/H_4R antagonists may be useful drugs for the treatment of this disease (Thurmond et al., 2008). Our finding that the combination of an H_1R antagonist and an H_4R antagonist during the sensitization phase exhibits a synergistic reducing effect on eosinophilia in a murine asthma model strongly supports this hypothesis (Fig. 4).

In a previous study, [^{3}H]mepyramine bound to recombinant hH_4R expressed in HEK293 cells with a K_d value of 32 nM, corresponding to a pK_d of 7.50 (Nguyen et al., 2001). In our hands, mepyramine binds to hH_4R with a pK_i of 5.44 (Table 1) (i.e., with an affinity that is 2 orders of magnitudes lower that reported by Nguyen et al. (2001). Similar differences between our results and those of Nguyen et al. (2001) (Table 1) were found for doxepine. However, for chlorpheniramine, our data and those from Nguyen et al. (2001) (Table 1) are in close agreement. Other groups (Lim et al., 2005; Venable and Thurmond, 2006) could not confirm the high-affinity binding of H_1R antagonists observed by Nguyen et al. (2001) as well. One possibility to reconcile the divergent data is that the HEK293 cells used by Nguyen et al. (2001) also (endogenously) expressed H_1R (Venable and Thurmond, 2006), exhibiting high affinity for mepyramine (pK_d 8.34) (Seifert et al., 2003). This value still differs from the value reported by Nguyen et al. (2001) by 1 order of magnitude, but a close analysis of the saturation binding experiment shown by Nguyen et al. (2001) in Fig. 4B of their article suggests that their system actually contains both high- and low-affinity mepyramine binding sites that were not analyzed appropriately with a two-site model. The putative low-affinity mepyramine binding site in the study of Nguyen, potentially corresponding to hH_4R, does not reach saturation. Moreover, the Hill slopes for many H_1R antagonists in the competition experiments shown in Fig. 5 and Table 1 of the article by Nguyen et al. (2001) are <1, indicating the presence of two binding sites that again were not resolved by a two-site model. We have no evidence for the presence of contaminating hH_1R in hH_4R-RGS19 membrane preparations as revealed by the lack of the typical immunoreactivity of hH_1R with the M1 monoclonal antibody (Seifert et al., 2003; Schneider and Seifert, 2009), lack of specific [^{3}H]mepyramine binding to hH_4R-RGS19 (data not shown), and lack of shallow and potentially biphasic competition isotherms (Table 1 and Fig. 5A).

Another possibility to explain the differences between our study and that of Nguyen et al. (2001) is that we studied hH_4R expressed in Sf9 insect cells, whereas they studied hH_4R expressed in a mammalian expression system. These differences in expression system could affect receptor glycosylation and oligomerization that, in turn, could affect the pharmacological GPCR properties. However, we verified that a number of prototypical hH_4R ligands exhibit very similar interactions with hH_4R expressed in Sf9 insect cells and mammalian cells (Lim et al., 2005; Schneider and Seifert, 2009; Schneider et al., 2009). Moreover and in agreement with our data, Lim et al. (2005) showed that several first- and second generation H_1R antagonists bind to hH_4R expressed in mammalian cells with pK_i values <5. Thus, we conclude that despite the confusion caused by the study of Nguyen et al. (2001), many first-generation H_1R antagonists (**1–8**), second-generation H_1R antagonists (**9–14**), and antidepressants (**16–18**) do bind to hH_4R, although with rather low affinity. Our data also suggest that previously reported therapeutic effects of first- and second-generation H_1R antagonists in type I allergic reactions (Thurmond et al., 2008) could be caused by dual blockade of both H_1R and H_4R. Assessment of in vivo drug concentrations would be required to test this hypothesis.

The low potency of astemizole in the GTPase assay contrasts with the substantially higher affinity of the compound in the competition binding experiments. Most likely, the competition binding assay and the GTPase assay monitor different GPCR states (i.e., the radioligand-occupied receptor state versus the ligand-free state, which may exhibit different affinities for various ligand classes). Similar differences between the competition binding and GTPase assay were observed for dimeric histaprodifen and several phenylhistamines, whereas for suprahistaprodifen, pK_i and pEC_{50} values match well. All these data lend support to the existence of ligand-specific hH_4R states. Evidence for ligand-specific GPCR conformations was already obtained for hH_1R and hH_2R (Seifert et al., 2003; Preuss et al., 2007; Strasser et al., 2008a,b, 2009).

Phenylhistamines show a different pharmacological profile at hH_1R and hH_4R. For phenylhistamines, moderately higher potency was observed at hH_1R compared with hH_4R (Fig. 7A). The different interaction of 2-phenylhistamines with hH_1R and hH_4R is reflected by a linear correlation of the pEC_{50} values that is shifted toward the right relative to the theoretical correlation describing pharmacological identity between hH_1R and hH_4R. Phenylhistamines are partial agonists at hH_1R and hH_4R (Fig. 7C). For the phenylhistamines, the efficacies are either in the same range at both hH_1R and hH_4R or higher at hH_1R that at hH_4R. Collectively, 2-phenylhistamines are less selective H_1R agonists than originally assumed (Leschke et al., 1995; Seifert et al., 2003). Future studies will have to determine whether the previously reported H_1R and H_2R antagonist-resistant effects of 2-phenylhistamines in HL-60 leukemia cells are mediated by hH_4R rather than by the originally assumed receptor-independent direct G-protein activation (Seifert et al., 1994).

As for phenylhistamines, differences in pharmacology between hH_1R and hH_4R were observed for the histaprodifens. Histaprodifens show higher potency at hH_1R compared with hH_4R (Fig. 7B). The linear correlation of the pEC_{50} values is shifted toward the right relative to the theoretical correlation describing pharmacological identity between hH_1R and hH_4R (Fig. 7B). This indicates different interactions of histaprodifens with hH_1R and hH_4R. However, in contrast to the phenylhistamines, only suprahistaprodifen is a partial agonist at hH_1R and hH_4R. All other histaprodifens are partial agonists at hH_1R but inverse agonists at hH_4R (Fig. 7C).

In molecular dynamics simulations, we found two stable binding modes for suprahistaprodifen at hH_4R (Fig. 6). In orientation 1, suprahistaprodifen stabilizes the inactive state of the hH_4R as a result of an interaction of one phenyl moiety of the diphenylpropyl moiety with $Trp^{6.48}$ in vertical conformation (Fig. 6A). The vertical conformation is typical for the inactive receptor state (Crocker et al., 2006). Because of the interaction with the phenyl moiety of the diphenyl group, $Trp^{6.48}$ is not able to switch into its horizontal conformation

(Fig. 6B), which is characteristic for the active state of the receptor (Crocker et al., 2006). In contrast, the molecular dynamics simulations found a stable active suprahistaprodifen-hH_4R complex when suprahistaprodifen is bound in orientation 2. There, $Trp^{6.48}$ is in a more horizontal, active conformation. Therefore, the rotamer toggle switch (Crocker et al., 2006), including $Trp^{6.48}$, can take place only for suprahistaprodifen bound in orientation 2 but not in orientation 1. Considering the results of the molecular dynamics study, we suggest that suprahistaprodifen can bind in to hH_4R in two orientations. Furthermore, we suggest that suprahistaprodifen acts as inverse agonist in orientation 1 and as partial agonist in orientation 2. Because a net increase in GTP hydrolysis is found with suprahistaprodifen, E_{max} resulting from the partial agonistic effect of suprahistaprodifen is larger than the E_{max} resulting from the inverse agonistic effect.

[^{35}S]Guanosine 5′-[γ-thio]triphosphate binding experiments with Sf9 membranes coexpressing hH_4R with $G\alpha_{i2}$ and membranes expressing only $G\alpha_{i2}$ without hH_4R predicted that, in contrast to the generally hold notion (Thurmond et al., 2008), thioperamide is not a full inverse agonist but only a partial inverse agonist (Schneider et al., 2008). In accordance with this prediction, dimeric histaprodifen was serendipitously found to inhibit GTP hydrolysis more effectively than thioperamide. Thus, dimeric histaprodifen stabilizes the inactive (R) state of the receptor more effectively than thioperamide. Furthermore, dimeric histaprodifen stabilizes the inactive conformation of hH_4R more effectively than methylhistaprodifen. It can be concluded that the second histaprodifen moiety in dimeric histaprodifen stabilizes the inactive conformation of the histaprodifen partial structure in the histaprodifen binding-pocket near TM5 and TM6 (Fig. 6). The small histaprodifens (e.g., compound **37**) should be more flexible in the histaprodifen binding-pocket near TM5 and TM6 (Fig. 6), resulting in a weaker stabilization of the inactive conformation compared with the bulky dimeric histaprodifen. It is possible that histaprodifens with even higher inverse agonistic activity than dimeric histaprodifen will be identified. Thus, in more general terms for constitutive GPCR activity (Seifert and Wenzel-Seifert, 2002), our studies highlight the difficulties in defining a "full" inverse agonist.

In conclusion, we have shown that H_1R antagonists and H_1R agonists bind to hH_4R with lower affinity than to hH_1R. H_1R ligands act as partial agonists, neutral antagonists, or inverse agonists. Astemizole, possessing some similarity with JNJ 7777120, is a good starting point for the development of dual H_1R/H_4R antagonists. Such compounds may be very useful for the treatment of type I allergies. Dimeric

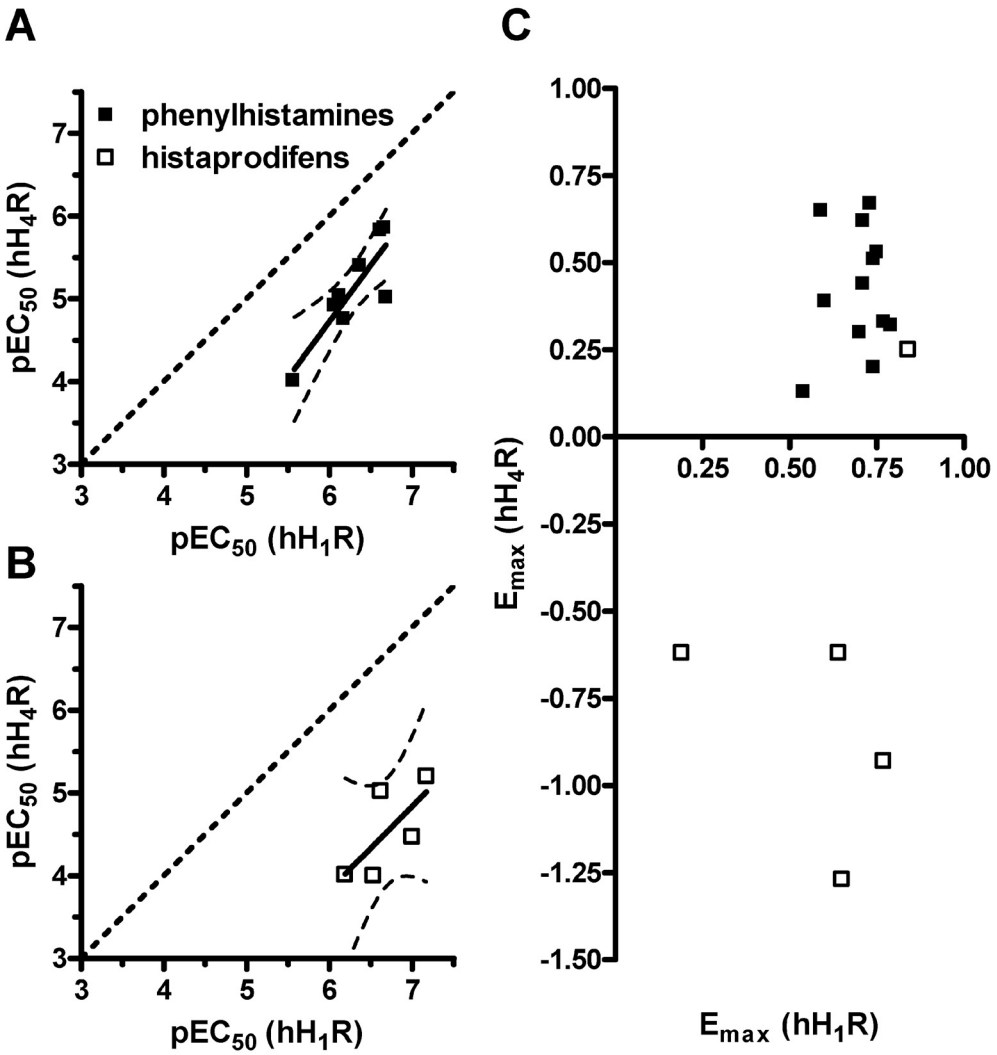

Fig. 7. Relations between the potencies or efficacies of phenylhistamines and histaprodifens between hH_1R and hH_4R in the steady-state GTPase assay. The straight short dashed lines represent the theoretical correlations, describing pharmacological identity between hH_1R and hH_4R. Relation between the pEC_{50} values was analyzed by linear regression. Solid lines represent the actual correlation. Long dashed lines represent the 95% confidence intervals of the correlation. A, correlation of the pEC_{50} values of phenylhistamines at hH_1R versus hH_4R. Slope, 1.36 ± 0.33; r^2, 0.74. B, correlation of the pEC_{50} values of histaprodifens at hH_1R versus hH_4R. pEC_{50} of compound **39** was set to 4. Slope, 1.01 ± 0.59; r^2, 0.50. C, relation of efficacies of phenylhistamines and histaprodifens between hH_1R and hH_4R.

histaprodifen surpasses thioperamide as an hH_4R inverse agonist in terms of efficacy. Accordingly, dimeric histaprodifen is an excellent starting point for the development of potent, selective and efficacious hH_4R inverse agonists. Such compounds may be of great value in the treatment of type I allergic diseases, too.

Acknowledgments

We thank A. Seefeld for performing some GTPase assays, G. Wilberg for competent help with the cell culture, and Dr. R. Thurmond (Johnson and Johnson Research and Development, La Jolla, CA) for providing JNJ 7777120. Thanks are also due to Dr. T. Tschernig (Institute of Functional and Applied Anatomy, Medical School of Hannover, Hannover, Germany) for his competent advice for the establishment of the acute murine asthma model and the reviewers for their thoughtful and constructive critique.

References

Ballesteros JA, Shi L, and Javitch JA (2001) Structural mimicry in G protein-coupled receptors: implications of the high-resolution structure of rhodopsin for structure-function analysis of rhodopsin-like receptors. *Mol Pharmacol* **60:**1–19.

Bruysters M, Jongejan A, Gillard M, van de Manakker F, Bakker RA, Chatelain P, and Leurs R (2005) Pharmacological differences between human and guinea pig histamine H_1 receptors: Asn^{84} (2.61) as a key residue within an additional binding pocket in the H_1 receptor. *Mol Pharmacol* **67:**1045–1052.

Cherezov V, Rosenbaum DM, Hanson MA, Rasmussen SG, Thian FS, Kobilka TS, Choi HJ, Kuhn P, Weis WI, Kobilka BK, et al. (2007) High-resolution crystal structure of an engineered human β_2-adrenergic G protein-coupled receptor. *Science* **318:**1258–1265.

Crocker E, Eilers M, Ahuja S, Hornak V, Hirshfeld A, Sheves M, and Smith SO (2006) Location of Trp265 in metarhodopsin II: implications for the activation mechanism of the visual receptor rhodopsin. *J Mol Biol* **357:**163–172.

Dunford PJ, O'Donnell N, Riley JP, Williams KN, Karlsson L, and Thurmond RL (2006) The histamine H_4 receptor mediates allergic airway inflammation by regulating the activation of $CD4^+$ T cells. *J Immunol* **176:**7062–7070.

Elz S, Kramer K, Pertz HH, Detert H, ter Laak AM, Kühne R, and Schunack W (2000) Histaprodifens: synthesis, pharmacological in vitro evaluation, and molecular modeling of a new class of highly active and selective histamine H_1-receptor agonists. *J Med Chem* **43:**1071–1084.

Foord SM, Bonner TI, Neubig RR, Rosser EM, Pin JP, Davenport AP, Spedding M, and Harmar AJ (2005) International Union of Pharmacology. XLVI. G protein-coupled receptor list. *Pharmacol Rev* **57:**279–288.

Gantz I, Munzert G, Tashiro T, Schäffer M, Wang L, DelValle J, and Yamada T (1991) Molecular cloning of the human histamine H_2 receptor. *Biochem Biophys Res Commun* **178:**1386–1392.

Hashimoto T, Harusawa S, Araki L, Zuiderveld OP, Smit MJ, Imazu T, Takashima S, Yamamoto Y, Sakamoto Y, Kurihara T, et al. (2003) A selective human H_4-receptor agonist: (−)-2-cyano-1-methyl-3-[(2*R*,5*R*)-5-[1*H*-imidazol-4(5)-yl]tetrahydrofuran-2-yl]methylguanidine. *J Med Chem* **46:**3162–3165.

Igel P, Schneider E, Schnell D, Elz S, Seifert R, and Buschauer A (2009) N^G-acylated imidazolylpropylguanidines as potent histamine H_4 receptor agonists: selectivity by variation of the N^G-substituent. *J Med Chem* **52:**2623–2627.

Jablonowski JA, Grice CA, Chai W, Dvorak CA, Venable JD, Kwok AK, Ly KS, Wei J, Baker SM, Desai PJ, et al. (2003) The first potent and selective non-imidazole human histamine H_4 receptor antagonist. *J Med Chem* **46:**3957–3960.

Jójárt B, Kiss R, Viskolcz B, and Keseru GM (2008) Activation mechanism of the human histamine H_4 receptor—an explicit membrane molecular dynamics simulation study. *J Chem Inf Model* **48:**1199–1210.

Jongejan A, Lim HD, Smits RA, de Esch IJ, Haaksma E, and Leurs R (2008) Delineation of agonist binding to the human histamine H_4 receptor using mutational analysis, homology modeling, and *ab initio* calculations. *J Chem Inf Model* **48:**1455–1463.

Kramer K, Elz S, Pertz HH, and Schunack W (1998) N^α-alkylated derivatives of 2-phenylhistamines: synthesis and in vitro activity of potent histamine H_1-receptor agonists. *Bioorg Med Chem Lett* **8:**2583–2588.

Leschke C, Elz S, Garbarg M, and Schunack W (1995) Synthesis and histamine H_1 receptor agonist activity of a series of 2-phenylhistamines, 2-heteroarylhistamines, and analogues. *J Med Chem* **38:**1287–1294.

Lezoualc'h F, Jockers R, and Berque-Bestel I (2009) Multivalent-based drug design applied to serotonin 5-HT_4 receptor oligomers. *Curr Pharm Des* **15:**719–729.

Lim HD, van Rijn RM, Ling P, Bakker RA, Thurmond RL, and Leurs R (2005) Evaluation of hstamine H_1-, H_2-, and H_3-receptor ligands at the human histamine H_4 receptor: identification of 4-methylhistamine as the first potent and selective H_4 receptor agonist. *J Pharmacol Exp Ther* **314:**1310–1321.

Lovenberg TW, Roland BL, Wilson SJ, Jiang X, Pyati J, Huvar A, Jackson MR, and Erlander MG (1999) Cloning and functional expression of the human histamine H_3 receptor. *Mol Pharmacol* **55:**1101–1107.

Menghin S, Pertz HH, Kramer K, Seifert R, Schunack W, and Elz S (2003) N^α-Imidazolylalkyl and pyridylalkyl derivatives of histaprodifen: synthesis and in vitro evaluation of highly potent histamine H_1-receptor agonists. *J Med Chem* **46:**5458–5470.

Moguilevsky N, Varsalona F, Noyer M, Gillard M, Guillaume JP, Garcia L, Szpirer C, Szpirer J, and Bollen A (1994) Stable expression of human H_1-histamine-receptor cDNA in Chinese hamster ovary cells. Pharmacological characterisation of the protein, tissue distribution of messenger RNA and chromosomal localisation of the gene. *Eur J Biochem* **224:**489–495.

Nguyen T, Shapiro DA, George SR, Setola V, Lee DK, Cheng R, Rauser L, Lee SP, Lynch KR, Roth BL, et al. (2001) Discovery of a novel member of the histamine receptor family. *Mol Pharmacol* **59:**427–433.

Niv MY, Skrabanek L, Filizola M, and Weinstein H (2006) Modeling activated states of GPCRs: the rhodopsin template. *J Comput Aided Mol Des* **20:**437–448.

Oda T, Morikawa N, Saito Y, Masuho Y, and Matsumoto S (2000) Molecular cloning and characterization of a novel type of histamine receptor preferentially expressed in leukocytes. *J Biol Chem* **275:**36781–36786.

Oostenbrink C, Villa A, Mark AE, and van Gunsteren WF (2004) A biomolecular force field based on the free enthalpy of hydration and solvation: the GROMOS force-field parameter sets 53A5 and 53A6. *J Comput Chem* **25:**1656–1676.

Preuss H, Ghorai P, Kraus A, Dove S, Buschauer A, and Seifert R (2007) Point mutations in the second extracellular loop of the histamine H_2 receptor do not affect the species-selective activity of guanidine-type agonists. *Naunyn Schmiedebergs Arch Pharmacol* **376:**253–264.

Rasmussen SG, Choi HJ, Rosenbaum DM, Kobilka TS, Thian FS, Edwards PC, Burghammer M, Ratnala VR, Sanishvili R, Fischetti RF, et al. (2007) Crystal structure of the human β_2 adrenergic G-protein-coupled receptor. *Nature* **450**:383–387.

Rosenbaum DM, Cherezov V, Hanson MA, Rasmussen SG, Thian FS, Kobilka TS, Choi HJ, Yao XJ, Weis WI, Stevens RC, et al. (2007) GPCR engineering yields high-resolution structural insights into β_2-adrenergic receptor function. *Science* **318:**1266–1273.

Schneider EH and Seifert R (2009) Histamine H_4 receptor-RGS fusion proteins expressed in Sf9 insect cells: a sensitive and reliable approach for the functional characterization of histamine H_4 receptor ligands. *Biochem Pharmacol* **78:**607–616.

Schneider EH, Schnell D, Papa D, and Seifert R (2009) High constitutive activity and a G-protein-independent high-affinity state of the human histamine H_4-receptor. *Biochemistry* **48:**1424–1438.

Seifert R and Wenzel-Seifert K (2002) Constitutive activity of G-protein-coupled receptors: cause of disease and common property of wild-type receptors. *Naunyn Schmiedebergs Arch Pharmacol* **366:**381–416.

Seifert R, Hagelüken A, Höer A, Höer D, Grünbaum L, Offermanns S, Schwaner I, Zingel V, Schunack W, and Schultz G (1994) The H_1 receptor agonist 2-(3-chlorophenyl)histamine activates G_i-proteins in HL-60 cells through a mechanism that is independent of known histamine receptor subtypes. *Mol Pharmacol* **45:**578–586.

Seifert R, Wenzel-Seifert K, Burckstummer T, Pertz HH, Schunack W, Dove S, Buschauer A, and Elz S (2003) Multiple differences in agonist and antagonist pharmacology between human and guinea pig histamine H_1-receptor. *J Pharmacol Exp Ther* **305:**1104–1115.

Smits RA, de Esch IJ, Zuiderveld OP, Broeker J, Sansuk K, Guaita E, Coruzzi G, Adami M, Haaksma E, and Leurs R (2008) Discovery of quinazolines as histamine H_4 receptor inverse agonists using a scaffold hopping approach. *J Med Chem* **51:**7855–7865.

Strasser A and Wittmann HJ (2007) Analysis of the activation mechanism of the guinea-pig histamine H_1-receptor. *J Comput Aided Mol Des* **21:**499–509.

Strasser A, Striegl B, Wittmann HJ, and Seifert R (2008a) Pharmacological profile of histaprodifens at four recombinant histamine H_1 receptor species isoforms. *J Pharmacol Exp Ther* **324:**60–71.

Strasser A, Wittmann HJ, and Seifert R (2008b) Influence of the N terminus and E2-loop to pharmacological properties of the histamine H_1-receptor. *J Pharmacol Exp Ther* **326:**783–791.

Strasser A, Wittmann HJ, Kunze M, Elz S, and Seifert R (2009) Molecular basis for the selective interaction of synthetic agonists with the human histamine H_1-receptor compared with the guinea-pig H_1-receptor. *Mol Pharmacol* **75:**454–465.

Terzioglu N, van Rijn RM, Bakker RA, De Esch IJ, and Leurs R (2004) Synthesis and structure-activity relationships of indole and benzimidazole piperazines as histamine H_4 receptor antagonists. *Bioorg Med Chem Lett* **14:**5251–5256.

Thurmond RL, Gelfand EW, and Dunford PJ (2008) The role of histamine H_1 and H_4 receptors in allergic inflammation: the search for new antihistamines. *Nat Rev Drug Discov* **7:**41–53.

Venable JD, Cai H, Chai W, Dvorak CA, Grice CA, Jablonowski JA, Shah CR, Kwok AK, Ly KS, Pio B, et al. (2005) Preparation and biological evaluation of indole, benzimidazole, and thienopyrrole piperazine carboxamides: potent human histamine h_4 antagonists. *J Med Chem* **48:**8289–8298.

Venable JD and Thurmond RL (2006) Development and chemistry of histamine H_4 receptor ligands as potential modulators of inflammatory and allergic responses. *Antiinflamm Antiallergy Agents Med Chem* **5:**307–322.

Address correspondence to: Dr. Roland Seifert, Institute of Pharmacology, Medical School of Hannover, Carl-Neuberg-Straße 1, D-30625 Hannover, Germany. E-mail: seifert.roland@mh-hannover.de